Proc. 11th Int. Conf. on Cosmic Rays, Budapest 1969

ZENITH-ANGLE DISTRIBUTION OF ULTRA-HIGH ENERGY MUONS*

J. W. KEUFFEL, J. L. OSBORNE,† G. L. BOLINGBROKE, G. W. MASON.‡
M. O. LARSON, G. H. LOWE, J. H. PARKER, R. O. STENERSON,
H. E. BERGESON

University of Utah, Salt Lake City, Utah 84112, U.S.A.

The intensity of muons was studied as a function of zenith angle at fixed slant depth of rock. Detailed studies of the uniformity of the rock and of the detector efficiencies show that there are no errors from these sources large enough to affect the angular dependence significantly. The results confirm our earlier conclusion that a direct muon production process does exist at about the 2% level.

Introduction

The zenith-angle distribution of ultra-high energy muons is of great importance because, in the conventional picture of high-energy interactions, the dominant source of muons is the decay of pions and kaons; and the competition between decay and capture of these parent particles produces an enhancement of the muon intensity at large zenith angles which is a definite, testable consequence of the theory. Evidence that an appreciable component of the muons above 10^{12} eV does not show this enhancement has already been presented by the Utah group [1, 2]. This paper reports the first results with the complete Utah underground detector. The statistical sample is large enough to permit a direct study of the intensity vs. zenith angle θ at fixed depths, eliminating in this way any dependence on the average density of the rock and of vertical intensities measured by other experimenters.

Since the present results are in agreement with the magnitude of the direct muon production component indicated by the most recent Utah results [2], the production model discussed there is still valid and the present paper will not discuss models but will confine itself to the presentation of results supporting the existence of direct muon production.

Enhancement factor

It will be useful to define an enhancement factor $G(h, q) = 1(h, q) / I(h, q)$ where $I(h, q)$ is the intensity of muons at angle q and *slant* depth h. Almost all the dependence of $I(h, q)$ on h is contained in the vertical intensity factor $I(h, 0)$, so that $G(h, q)$

*Supported by the National Science Foundation, U.S.A.

†Present address: University of Durham, Durham, England.

‡Present address: Brigham Young University, Provo, Utah, U.S.A.

is a mildly-varying function of *h*, as may be seen from Fig. 1. Consequently, it is permissible to group together data obtained at the same *q* but different *h* by correcting each point according to the vertical depth-intensity curve* over intervals of < 400 hg/cm^2 without incurring errors >2-3% whatever model is used.

This mild dependence on *h* may easily be understood physically, since for the conventional model (R = 0) the angular dependence of the muon intensity derives from the "competition factor" *B/(E cos q + B)*, and the enhancement factor

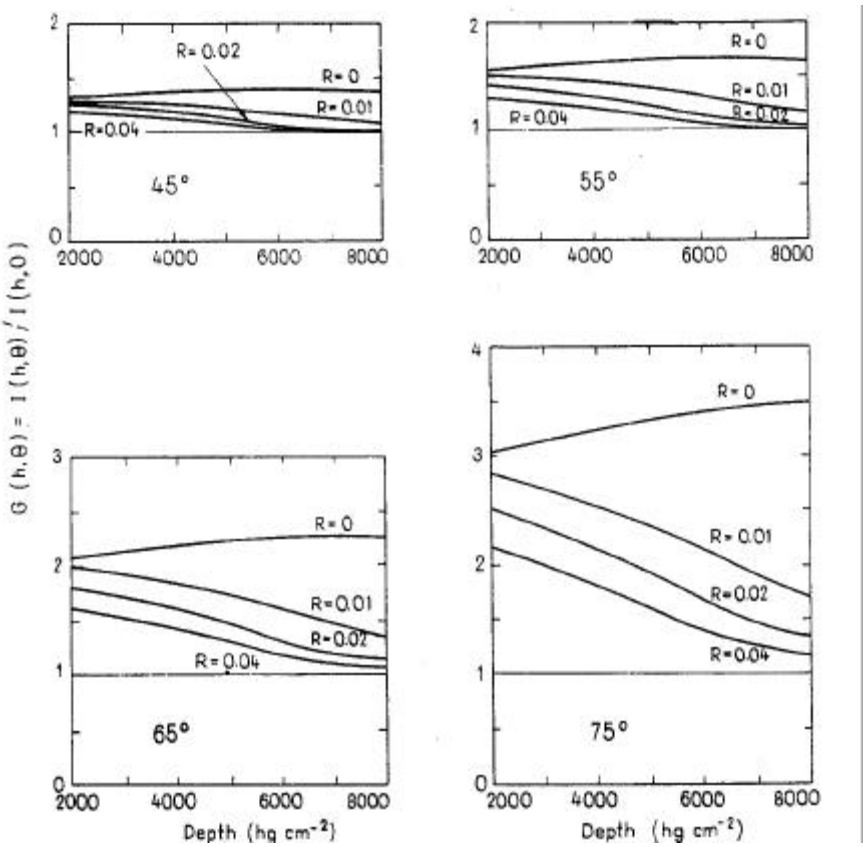

Fig. 1. Enhancement factors G(h, 0) predicted on the basis of various models. A 20% admixture of kaons has been included for all curves. R is the fraction of X-process muons relative to pions of the same energy at production

approaches the conventional sec *q*, independent of *h*, for muon energies *E* > *B* - *a* condition which is well satisfied at our depths for muons of pion parentage (B_p = 90 GeV). On the other hand, in a model which incorporates an admixture of directly-produced muons, the enhancement factor approaches unity (also independent of *h)* at high energies and, at intermediate energies, the transition from pion to X-process parentage is gradual.

* Our adopted world-survey depth-intensity curve is the same as used in [1] and [2].

In the curves of Fig. 1, the parameter *R* is the ratio of X-process muons to pions produced at the same energy, and the enhancement functions, although rigorously calculated with the inclusion of fluctuations in the muon ranges, do not differ to any large extent from the enhancement factor for the differential muon spectrum $(BE^{-1} \sec\theta + R)/(BE^{-1} + R)$ provided a suitable average energy corresponding to the depth *h* is inserted. Thus the main conclusions of this paper are not sensitive to the details of the calculation of G(h, θ).

Apparatus

The Utah neutrino detector consists of a 6 x 10 x 12 m^3 array of sonic cylindrical spark counters and Cerenkov detectors. There are four Cerenkov detectors in the form of vertical 6 x 10 m^2 x 3 m thick tanks filled with water. Fast coincidences between any two tanks trigger the spark counter array, and information from the sonic recording system is stored on magnetic tape in a convenient form for analysis and reconstruction by computer. To trigger the apparatus and to be accepted by the scanning, a muon must have had an energy of about 2 GeV and must have traversed 10 geometrical free paths of concrete and iron in a straight line.

Intensity vs. zenith angle

Each muon satisfying certain fiducial criteria was assigned to a 2.5° x 5° zenithazimuth bin. Because of the mountainous overburden, the effective slant depth, , depends on azimuth as well as zenith angle θ. We pick out all the bins with depths lying within ± 400 hg/cm^2 of certain central values and treat the data within them as follows. First, the raw number of muons is corrected for the Cerenkov tank efficiency and for the depth-intensity ratio relative to the central depth value. The muon intensity in that depth band for each 2.5° range of θ is then computed by dividing the corrected number of muons by the sum of the apertures (area-solid angle factors) computed for each bin and by the running time.

During a run of 7.65 x 10^6 sec live time, 92 945 muons were observed which entered the useful aperture. The intensities as a function of sec θ* are plotted in Fig. 2 for six different values of *h*. (θ* is the zenith angle at the production layer of the atmosphere for a trajectory whose local angle is θ.) Straight line segments representing $\sec^s \theta^*$ have been fitted to the points, and a summary of the resulting s-values is shown. For comparison, we show also values of s obtained by taking the average slope of the 1 vs. sec θ* curves over the particular angular ranges accessible to our apparatus. The near-constancy of these s-values for a given *R* is a consequence of the fact that, for our apparatus, larger values of depth (and of E) tend to be associated with larger values of sec θ, and the enhancement is, roughly speaking, a function of sec θ/E.

The results are clearly inconsistent with the conventional picture of muon production. Before commenting further on the choice of a preferred model, we turn to a discussion of systematic errors.

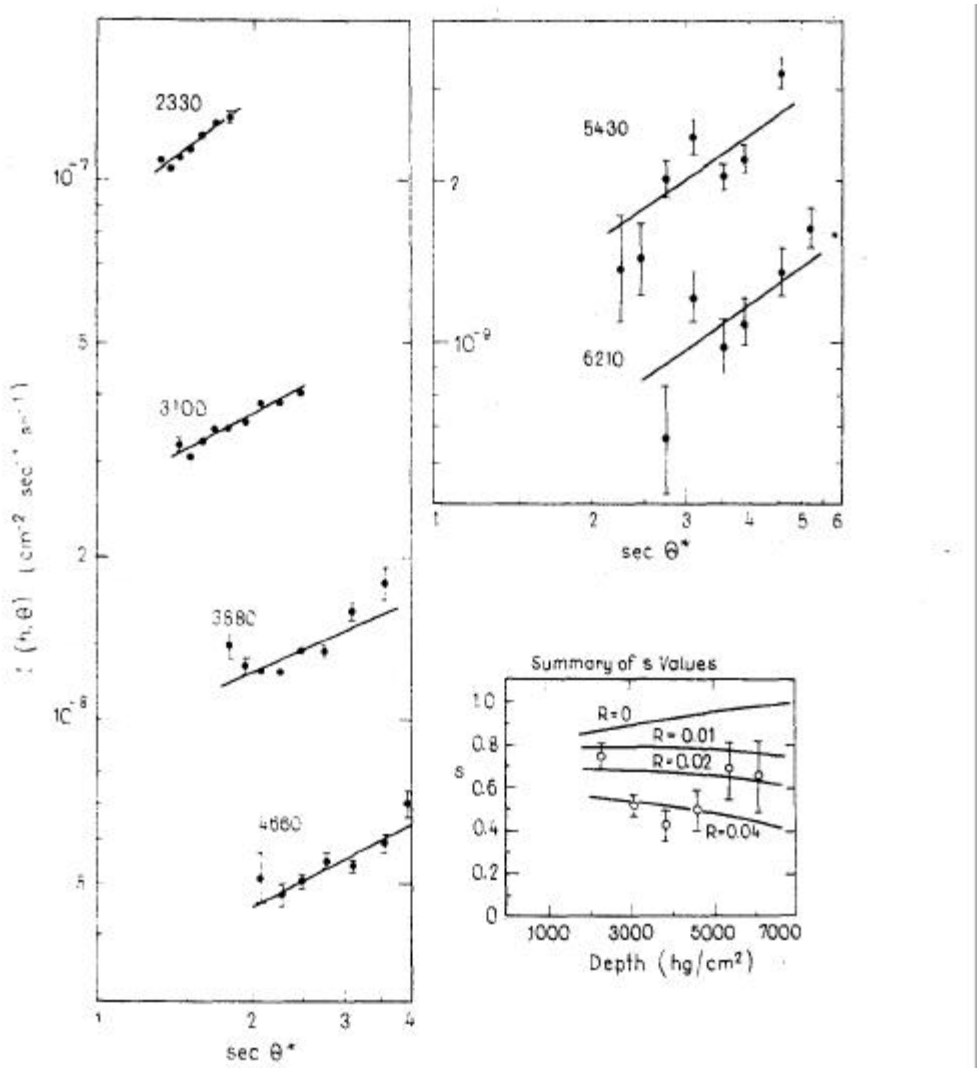

Fig. 2. Muon intensities vs. sec θ* at constant depth *h*. Line segments on the log-log plots have been fitted to the points, and the resulting slopes *s* are summarized, together with their statistical errors, in the lower right-hand corner. Also shown there are the *s*-values predicted for various values of R

Azimuthal uniformity

As one test of the uniformity of the surrounding rock, we adopted a procedure which is equivalent to comparing intensities observed at the same zenith angle and the same depth but at many different azimuths. The number of muons, corrected for efficiency, in each 5° x 20° zenith-azimuth bin was divided by the number of muons which would be expected in a bin of that aperture and at that *h* using our vertical depth-intensity relation. Enhancement factors obtained in this way are plotted in Fig. 3. The enhancements for a given range of θ should be constant except for a possible dependence of *G(h, q)* on *h* or for errors in the adopted vertical depth-intensity relation. The deviations from the mean for each θ-range vary from 10-15 %, implying (in view of the steep depth-intensity curve) density variations no greater than ± 2%.

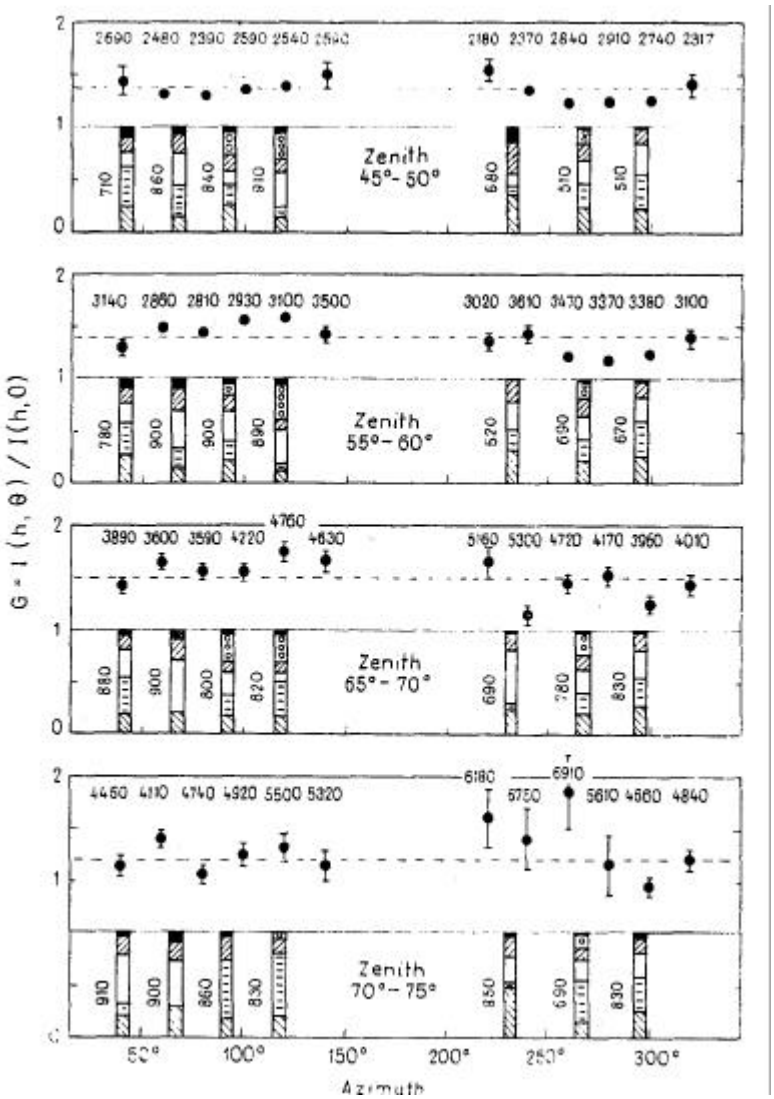

Fig. 3. Studies of azimuthal uniformity for representative zenith-angle ranges. Details of the method of computing the enhancement factors are given in the text. The mean depth for each point, in hg/cm^2, is shown directly above each point. The fractional compositions of the rock formations seen in given directions are shown as cross-hatched bars. Alongside these bars are shown the mean vertical overburdens, in hg/cm^2, for elements along the particular trajectories

Rock formations

As a second test of the uniformity of the surrounding rock, we measured the density of a large number of samples taken in three different general locations: one close up, one at 6000 ft, and one in between. There are four principal formations and one or two less common ones in the vicinity. For a number of zenith and azimuth angles, the fractions of the muon trajectory spent in each formation are shown as cross-hatched bars in Fig. 3. Most of the bars include a sizeable fraction of each formation.

Samples measured within a given formation showed a spread in densities of 2-4%, with occasional deviations as high as ± 10%. (The high-density samples are usually associated with mineralization and tend to be localized.) For the densities of the formations averaged over all our samples, we obtained the values 2.62, 2.56, 2.63, and 2.61. The averages over all the formations for the densities at the three locations - the quantities of greatest relevance here - were 2.56, 2.62, and 2.65 for the closest to the furthest away, respectively.

Thus the non-uniformities for typical runs of rock, estimated either from azimuthal variations or from direct measurements at different locations, are ±2%, too small to accommodate the 13% increase in density required between 40° and 75° zenith angles if our observations are to be reconciled with conventional muon production.

As a check on possible (but unlikely) compression effects on the density, the mean vertical overburden for elements of the trajectories analyzed in Fig. 3 is shown as a number alongside the bar. This parameter does not change very much with zenith angle, nor is there any correlation between it and the intensities. As for water content, our samples were all saturated and we measured all densities saturated. The mean values of Z^2 / A for our formations were 5.62, 5.62, 5.72, and 5.54; we took a weighted average of 5.65 and corrected our depth values to standard rock (Z^2 / A = = 5.5), a correction of 0.5 / 2 % over our range of depths.

Efficiencies

The four Èerenkov tanks of the complete detector, any two of which could trigger the event, permitted the efficiencies to be measured simultaneously with the actual runs. Even at steep zenith angles, muon showers provided the 3-tank events necessary for efficiency measurements. The efficiencies of the tanks were measured individually (each direction) as a function of the angle á of the muon to the normal to the tank, since the efficiencies were found to depend uniquely on á. Each muon trajectory was classified as a 2-tank, 3-tank, or 4-tank event according to the number of tanks traversed (regardless of which ones showed a trigger logic marker), and the efficiency was calculated.

The overall detector efficiencies, together with the percentages of 2-, 3-, and 4-tank events which contributed to the muon totals, are shown in Table 1. The fact that these efficiencies are so nearly constant, despite the fact that the efficiencies of single tanks drop as low as 50% for near-normal incidence,* is a consequence of two facts: first, there are very few normally incident muons in the data because of our ± 60° range in azimuth; and, second, the fraction of 3- and 4-tank muon trajectories is greatest where the individual tank efficiencies are least.

To test the sensitivity of our s-values to the dependence of the individual tank efficiency, we canted the efficiency vs. á curves so that they were 4 % high at large

* The tank efficiencies showed a steady deterioration over a period of two years from the high values of our first paper to the present. The deterioration is due to the aging of the photomultipliers, which are operated beyond their rated gains. Replacing the system with a stable, high efficiency one will be undertaken as soon as financial support is available.

Table 1
Overall detection efficiencies
Entries are percent efficiencies followed, in parentheses,
by the proportions 2-tank : 3-tank : 4-tank events

Zenith angle	Azimuth (4 quadrants consolidated, 0° = normal)		
	0°–20°	20°–40°	40°–60°
40°—45°	64.0(100 : 0 : 0)	62.5(100 : 0 : 0)	66.5(100 : 0 : 0)
45°—50°	63.5(100 : 0 : 0)	66.0(100 : 0 : 0)	64.0(100 : 0 : 0)
50°—55°	61.0(100 : 0 : 0)	65.0(100 : 0 : 0)	67.0(100 : 0 : 0)
55°—60°	62.0 (64 : 36 : 0)	66.0 (86 : 14 : 0)	69.0(100 : 0 : 0)
60°—65°	61.5 (41 : 55 : 4)	65.5 (62 : 37 : 1)	69.0 (95 : 5 : 0)
65°—70°	58.5 (31 : 47 : 22)	66.0 (52 : 39 : 9)	76.0 (87 : 13 : 0)
70°—75°	56.0 (22 : 38 : 40)	68.5 (43 : 39 : 18)	72.0 (81 : 19 : 0)
75°—80°	56.0 (17 : 30 : 53)	69.0 (40 : 35 : 25)	74.5 (64 : 32 : 4)

á and 4%. low at low á (very generous tolerances) and vice-versa. There was a negligible change in s-values except for the two lowest-depth s-values, which changed less than 5 %.

A further valuable check on efficiencies is afforded by azimuthal intensity tests of the sort shown in Fig. 3. In Table 2, we give the ratios $I(h, q)/I(h, 0)$ but with consolidation of azimuth sectors which are symmetrical to the detector. This procedure smoothes out the effects of terrain and brings out efficiency-dependent features. The intensities derived solely from 2-tank, 3-tank, and 4-tank events, where available, are given relative to the vertical intensity using appropriate apertures. A comparison of Table 2 and Fig. 3 shows the variations in intensities due to efficiency errors to be negligible compared with those due to non-uniformity in terrain. The consistency between the 2-tank, 3-tank, and 4-tank intensities is particularly reassuring.

Table 2
$I(h, q) / I(h, 0)$ for 2-tank, 3-tank, and 4-tank events

Zenith angle		Azimuth (4 quadrants consolidated, 0° = normal) 0°- 20°	20°- 40°	40°- 60°
40°- 50°	2-tank	1.26 ± 0.01	1.33 ± 0.01	1.46 ± 0.05
50°- 60°	2-tank	1.39 ± 0.01	1.43 ± 0.01	1.35 ± 0.02
	3-tank	1.36 ± 0.02	1.47 ± 0.05	
60°- 70°	2-tank	1.41 ± 0.02	1.46 ± 0.02	1.43 ± 0.03
	3-tank	1.47 ± 0.02	1.47 ± 0.03	1.49 ± 0.10
	4-tank	1.41 ± 0.05	1.61 ± 0.11	
70°- 80°	2-tank	1.56 ± 0.11	1.78 ± 0.06	1.68 ± 0.06
	3-tank	1.86 ± 0.10	1.82 ± 0.07	1.87 ± 0.13
	4-tank	1.73 ± 0.09	2.08 ± 0.11	

Combined enhancement plot

To gather together our measurements made at widely different depths and to compare our results with those of other workers, a best value for the mean density is needed. The average of our measured densities might be expected to be a trifle high, since our samples were obtained mostly at depth and in mine shafts and tunnels where mineralization is more likely to occur. Handbook values for our local formations based on widely distributed surface samples give a weighted average of 2.47 (the value used in our first paper) as compared with 2.61 for our measurements. We therefore tentatively adopted the value 2.54 and used this value in preparing Fig. 3 and Table 2 and in correcting intensities to the central values of Fig. 2. The conclusions drawn from these Figures are grossly insensitive to the mean density.

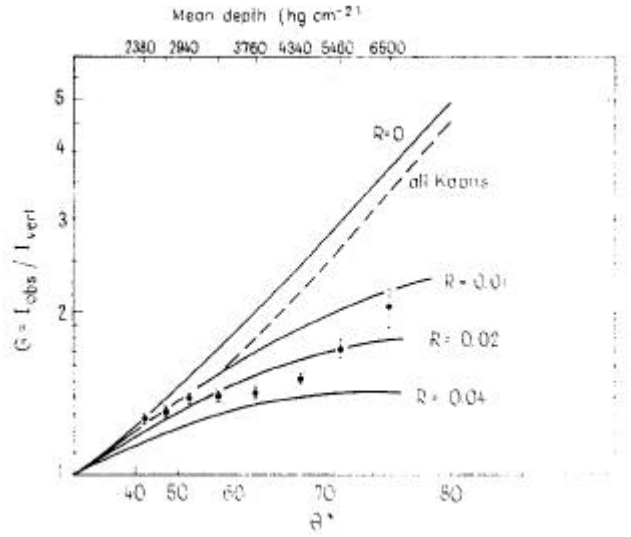

Fig. 4. Observed enhancements, averaged over azimuth, as a function of sec *()**. Each point is the weighted average G-value derived from sets of data such as are shown in Fig. 3. The flags are derived from the internal consistency of each such set of G-values. Also shown are the predictions of various models. The prediction for all kaons was made without regard to fluctuations in muon ranges and so is somewhat less accurate than the other curves; but it does, of course, take into account the muons from pion-decay modes of the charged and neutral kaons.

Experimental enhancement factors using this density, averaged over azimuth, are plotted against sec q^* in Fig. 4. Also shown are predictions of $G(h_{eff}, q)$ corresponding to various models, where h_{eff} is the mean value of the depth for that value of sec q^*. The prediction for all kaons took into account all K-decay modes. Although somewhat crude, the accuracy of this prediction is considered .adequate to exclude an all-kaon explanation of our observations. At the smallest zenith angles, where the predictions of all the models do not differ much, the experimental G-values agree with the curves, thus confirming our tentative choice of density. The flags in Fig. 4 are derived from the internal consistency of each set of 12 G-values; the statistical errors would be much smaller. Studies of scattering and angular errors, now under way, suggest that some reduction in the points at largest θ may be required.

The present results, especially the zenith-angle variations shown in Fig. 3, confirm our earlier conclusion that a new production process for ultra-high energy muons does exist, and at about the 2% level. The new results appear to indicate that the X-process percentage (the R parameter) goes through a broad maximum in the vicinity of 4000 hg/cm^2. Such an effect would be perfectly reasonable, either as the growth and decay of a particular process with energy, or as an effect due to a strongly interacting but weakly-decaying X-particle, for which the competition factor was merely delayed to very high energies because of a high mass or short mean life or both; but some variation in R could still be due to variations in rock density. Apart from this variation, the general analysis of BERGESON et al. [2] is applicable, including the necessity to invoke a larger value for the photonuclear interaction of muons.

Studies are under way to investigate experimentally the possibility that low energy photonuclear-produced pions could explain the discrepancies between our findings and those of KRISHNASWAMY et al. [3] and STOCKEL [4].

References

1. H. E. BERGESON, J. W. KEUFFEL, M. O. LARSON, E. R. MARTIN, G. W. MASON, Phys. Rev. Lett., 19, 1487, 1967.
2. H. E. BERGESON, J. W. KEUFFEL, M. O. LARSON, G. W. MASON, J. L. OSBORNE, Phys. Rev. Lett., 21, 1089, 1968.
3. M. R. KRISHNASWAMY, M. G. K. MENON, V. S. NARASIMHAM, S. KAWAKAMI, S. KING, S. MIYAKE, Phys. Lett., 27, 535, 1968.
4. C. T. STOCKEL, J. Phys. A, 2, 639, 1969.